Biocatalysis and Agricultural Biotechnology 23 (2020) 101455

Contents lists available at ScienceDirect

Biocatalysis and Agricultural Biotechnology

journal homepage: http://www.elsevier.com/locate/bab

In-depth spectral characterization of antioxidative (1,3)-β-D-glucan from the mycelium of an identified tiger milk mushroom *Lignosus rhinocerus* strain ABI in a stirred-tank bioreactor

Siti Rokhiyah Ahmad Usuldin [a, b], Norfaizah Mahmud [b], Zul Ilham [c, f], Nur Kusaira Khairul Ikram [d], Rahayu Ahmad [e], Wan Abd Al Qadr Imad Wan-Mohtar [b, f, *]

[a] Agro-Biotechnology Institute, Malaysia (ABI), National Institutes of Biotechnology Malaysia (NIMB), C/o HQ MARDI, 43400, Serdang, Selangor, Malaysia
[b] Mushroom Research Centre and Functional Foods and Bioprocess Development Laboratory, Institute of Biological Sciences, Faculty of Science, University of Malaya, 505603, Kuala Lumpur, Malaysia
[c] Biomass Energy Laboratory, Institute of Biological Sciences, Faculty of Science, University of Malaya, 50603, Kuala Lumpur, Malaysia
[d] Centre for Research in Biotechnology for Agriculture (CEBAR), University of Malaya, Kuala Lumpur, Malaysia
[e] Halal Action Laboratory, Pusat Genius Insan, University Sains Islam Malaysia, Bandar Baru Nilai, 71800, Nilai, Negeri Sembilan, Malaysia
[f] Bioresources and Bioprocessing Research Group, Institute of Biological Sciences, Faculty of Science, University of Malaya, 50603, Kuala Lumpur, Malaysia

ARTICLE INFO

Keywords:
Lignosus rhinocerus
Tiger milk mushroom
2D NMR
Bioreactor fermentation
(1,3)-β -D-glucan
Antioxidant

ABSTRACT

A rare Malaysian tiger milk mushroom *Lignosus rhinocerus* strain ABI (LRSA) was morphologically identified based on its pileus, stipe, and sclerotium. LRSA (515 bp) was sequenced and found to have 99% similar to *L. rhinocerus* strains CH31 and CH2. Phylogenetically, evolutionary distance (K_{nuc}) and plasmid-matching software (ApE) for sequences of matching fungal species were used to verify that the isolate belonged to the *L. rhinocerus* species. The strain was cultured in a stirred-tank bioreactor and a mycelial β-glucan (G) was extracted for compound characterization. The structure of exopolysaccharide extract from mycelium of LRSA was studied using Fourier-transform infrared spectroscopy (FT-IR) and one-dimensional (1D) and two-dimensional (2D) Nuclear Magnetic Resonance (NMR). FT-IR spectroscopy showed that G exhibited a similar β-glycosidic structure to the standard (laminarin), and the presence of characteristic bands at 3277, 2919, 1638, 1545, 1400, 1078, and 896 cm^{-1} confirmed the similarities. ^{1}H and ^{13}C NMR, as well as 2D NMR: homonuclear correlation spectroscopy (COSY), total correlation spectroscopy (TOCSY), heteronuclear multiple quantum coherence (HMQC), and heteronuclear multiple bond coherence (HMBC) spectra, were used for structural elucidation of the β-glucan and confirmed the extracted material as (1,3)-β-D-glucan. In addition, the G compound exhibited antioxidant activities through total phenolic content (4.47 mg gallic acid equivalents/g), 2, 2-diphenyl-1-picrylhydrazyl (11.48 mg/mL), and ferric reducing antioxidant power (0.56 mg/mL) assays. These findings may facilitate the development of rare G production in a high-scale bioreactor using LRSA.

1. Introduction

The tiger milk mushroom, scientifically known as *Lignosus rhinocerus (L. rhinocerus)*, is classified within the kingdom of fungi in the Basidiomycota division of the Polyporaceae family (Abdullah et al., 2013; Johnathan et al., 2016). The name of this mushroom derives from a folklore belief that the mushroom appears on the ground where the milk of a tigress has fallen (Fung and Tan, 2019). The tiger milk mushroom can be found in southern regions of China, Sri Lanka, Thailand, Philippines, Indonesia, Papua New Guinea, Australia, Vanuatu, and Malaysia (Cui et al., 2011; Núñez and Ryvarden, 2001). However, wild tiger milk mushroom is generally expensive and difficult to source because its natural abundance is low and it can only be found within areas with approximately a 5-km radius (Fung and Tan,

* Corresponding author. Mushroom Research Centre and Functional Foods and Bioprocess Development Laboratory, Institute of Biological Sciences, Faculty of Science, University of Malaya, 505603, Kuala Lumpur, Malaysia.
E-mail address: qadyr@um.edu.my (W.A.A.Q.I. Wan-Mohtar).

https://doi.org/10.1016/j.bcab.2019.101455
Received 21 August 2019; Received in revised form 6 November 2019; Accepted 27 November 2019
Available online 27 November 2019

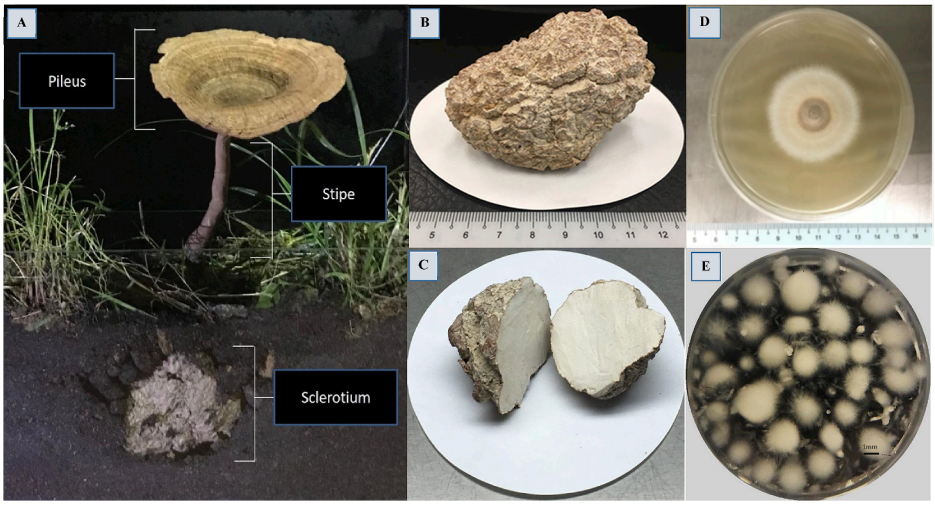

Fig. 1. Samples of *L. rhinocerus* from different developmental stages. (A) Basidiocarp of tiger milk mushroom isolated from a tropical forest in Lata Iskandar, Pahang, 4.3244° N, 101.3249° E, Malaysia. (B) Irregular shape sclerotium of *L. rhinocerus*, (C) Sliced sclerotium of *L. rhinocerus* (D) Mycelium of *L. rhinocerus* strain ABI on PDA medium at day 5 (E) Mycelium pellet of *L. rhinocerus* strain ABI at day 14.

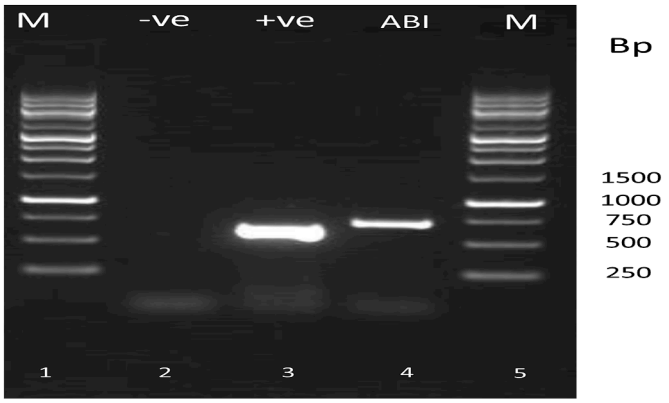

Fig. 2. Ethidium bromide fluorescence image showing electrophoresis of *Lignosus rhinocerus* strain ABI (LRSA) PCR product. The gel consists of 1% agarose and run with 1% TE buffer at 80 V. *Lanes 1 and 5* DNA marker; *Lane 2* PCR no template control; *Lane 3* positive control Fungal gDNA; *Lane 4* PCR ABI product.

2019). Furthermore, it can take months to locate the fruiting body from its emerged pileus above ground with the underground sclerotium (Yap et al., 2014).

This mushroom comprises a pileus (cap), stipe (stem), and sclerotium (tuber) (Nallathamby et al., 2018). The sclerotium of *L. rhinocerus* is the most important part of the mushroom and contains medicinal compounds with multiple properties for the treatment of diseases including cancer, cough, asthma, fever, and other ailments (Lau et al., 2015). Previous research has demonstrated that the sclerotia of *L. rhinocerus* possess immunomodulatory, anti-inflammatory, anti-oxidative, anti-proliferative, anti-microbial, anti-asthmatic, and anti-viral activities (Abdullah et al., 2011; Johnathan et al., 2016; Lee et al., 2014; Mohanarji et al., 2012; Wong et al., 2011; Yap et al., 2013). Of note, *L. rhinocerus* has frequently been confused with *Pleurotus tuber-regium* or *Lentinus tuber-regium* due to their similarities, including centrally stipitate basidiocarps (Nallathamby et al., 2018). The stipe alone might not be sufficient to morphologically characterize and phylogenetically differentiate the genus. Thus, molecular phylogenetic tree analysis is required to evaluate and classify the mushroom (Sotome et al., 2008).

The cultivation of tiger milk mushroom using solid state fermentation (SSF) is limited by factors including a longer duration required for the development of the tuber and fruiting body and slow mycelial growth. In addition, SSF is difficult to monitor, control, and scale up (Fazenda et al., 2008). Thus, submerged liquid fermentation (SLF) has become the preferred method for mycelial fermentation and commercial applications. Total polysaccharide produced in mushroom typically consists of exopolysaccharide (EPS) and intracellular polysaccharide (IPS) (Supramani et al., 2019a). EPS is excreted by the mycelium for survival under stress conditions while IPS is produced within the mycelium cell (Liu et al., 2010; Sathiyanarayanan et al., 2017). EPS is a high-molecular-weight polymer with a simple monosaccharide composition (Lai et al., 2014). The molecular weight (Mw) distributions of some fungal exopolysaccharides ranges from 13 kDa to 4.3 × 10^6 kDa (Mahapatra and Banerjee, 2013). For *L. rhinocerus*, the high molecular weight of its sclerotia polysaccharide was found to be more than 30 kDa (Yap et al., 2018). However, variations in molecular weight and sugar composition of fungal EPSs are dependent on many factors including strain, culture conditions, and medium composition (Rabha et al., 2012). The primary polysaccharide found in the *L. rhinocerus* cell wall is β-glucan, which comprises 65%–90% (1,3)-β-D-glucan (Bowman and Free, 2006; Lau et al., 2013a). β-glucan is made up of D-glucose monomers linked by β-glycosidic bonds and containing only glucose as a structural constituent (Ruthes et al., 2013). The biological effects of β-glucan are dependent on its primary structure, conformation, and molecular weight (Tada et al., 2009). The biological activity of β-glucan in basidiomycetes has been shown to exert a positive effect on the immune systems of both humans and animals (Rop et al., 2009). Thus, submerged fermentation of mycelium basidiomycetes is more efficient, reliable, reproducible, flexible, and easier to monitor compared with solid state fermentation of fruiting bodies, especially for the production of mycelial biomasses and their bioactive compounds, exopolysaccharides and other exo-biopolymers such as polysaccharide–protein complexes (Komura et al., 2010; Leung et al., 2009).

Oxidative stress caused by reactive oxygen species (ROS) can cause cellular damage and is thus implicated in a number of disorders such as aging, inflammation, atherosclerosis, and cancer (Kozarski et al., 2015). Recent interest in the development of effective and safe natural antioxidants highlights the importance of replacing synthetic antioxidants due to their side effects such as eczema, gastrointestinal upsets, cholesterol in blood, and hyperkinesis (Lidon and Silva, 2016). Hence, antioxidants isolated from natural sources such as mushrooms represent beneficial nutraceuticals and functional foods for health and disease prevention (Brewer, 2011; Kofuji et al., 2012; Munir et al., 2013; Wan-Mohtar et al., 2017). Several studies have shown the poly-

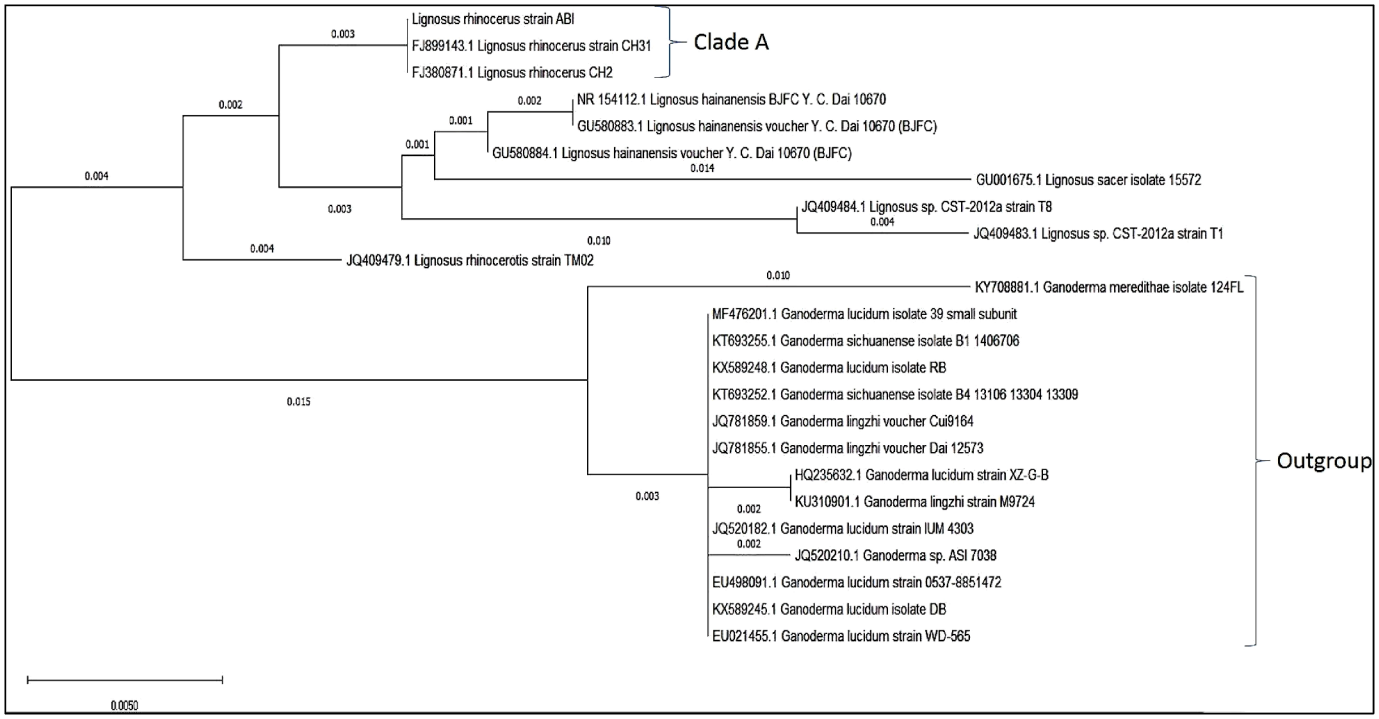

Fig. 3. Neighbour-joining phylogenetic tree showing the relationships of tiger milk mushroom *Lignosus rhinocerus* isolate 515bp (strain ABI) and top-9 BLAST species based on 18S rRNA gene sequences. The isolate located at clade A and evolutionary distance (K_{nuc}) was at 0.03 closest to *Lignosus rhinocerus*. *Bar* 0.0050.

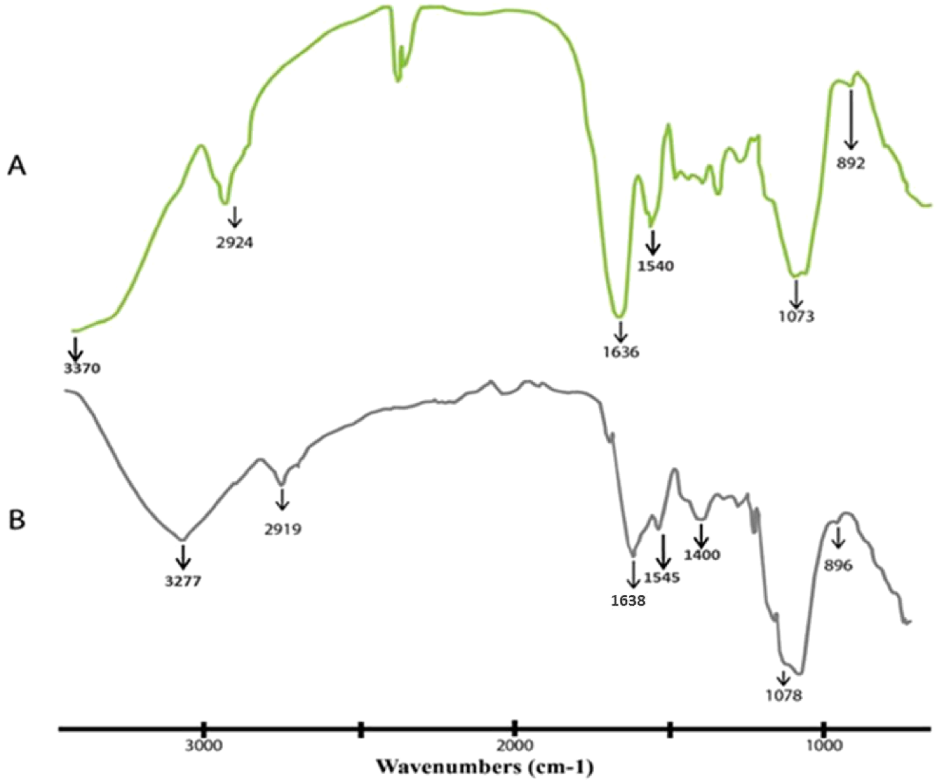

Fig. 4. Comparison of β-glucan IR spectra. A: standard glucan from laminarin (*Laminaria digitata*); B: glucan (G) derived from tiger milk mushroom *Lignosus rhinocerus* strain ABI (LRSA) mycelium.

saccharide fractions of the fruiting body and mycelial biomass of *L. rhinocerus* possess significant antioxidant activities (Jamil et al., 2018; Kong et al., 2016; Lau et al., 2014; Yap et al., 2013). However, the properties of exopolysaccharide produced in liquid or submerged fermentation for *L. rhinocerus* are not well characterized.

The objective of the present study was to isolate wild Malaysian tiger milk mushroom using morphological, polymerase chain reaction (PCR) molecular sequencing, phylogenetic Molecular Evolutionary Genetic Analysis (MEGA) software, and plasmid matching software methods. The isolated strain was cultured in a controlled bioreactor to

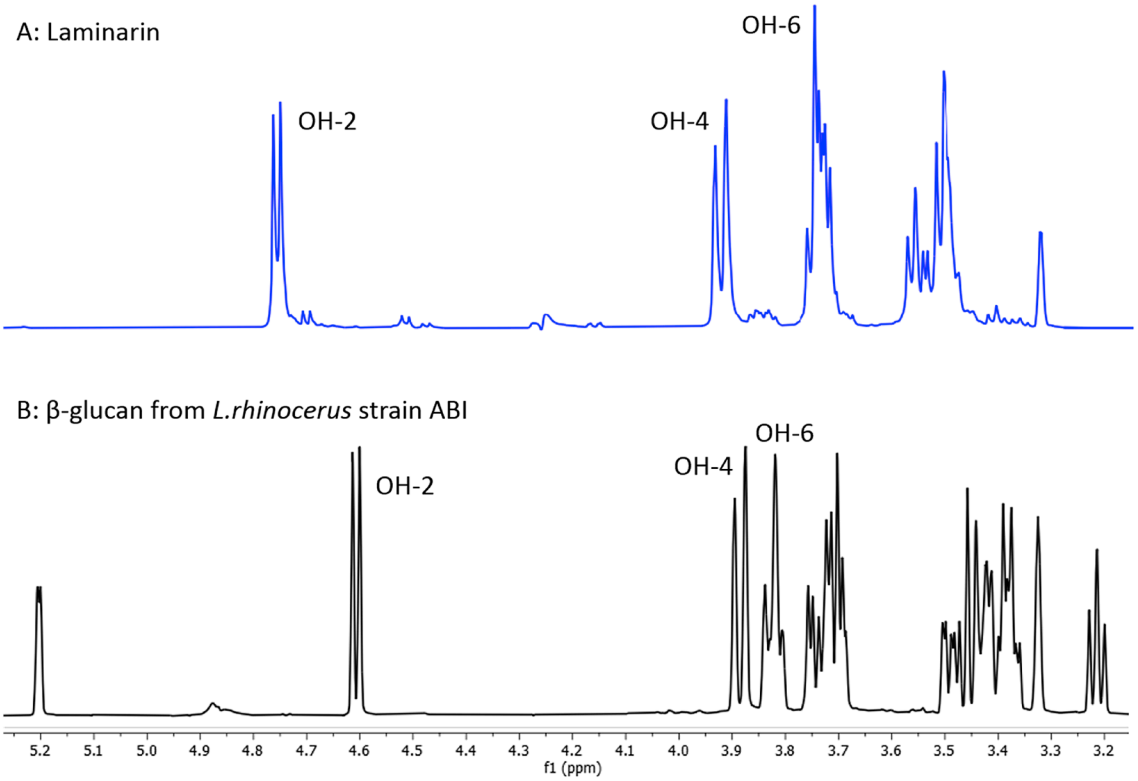

Fig. 5. ^{1}H NMR spectra of (1–3)-β-D-glucan. A: standard glucan from laminarin (*Laminaria digitata*) in D_20-d_6 at 80 °C; B: glucan (G) derived from batch cultures of tiger milk mushroom *Lignosus rhinocerus* strain ABI in D_20-d_6 at 25 °C.

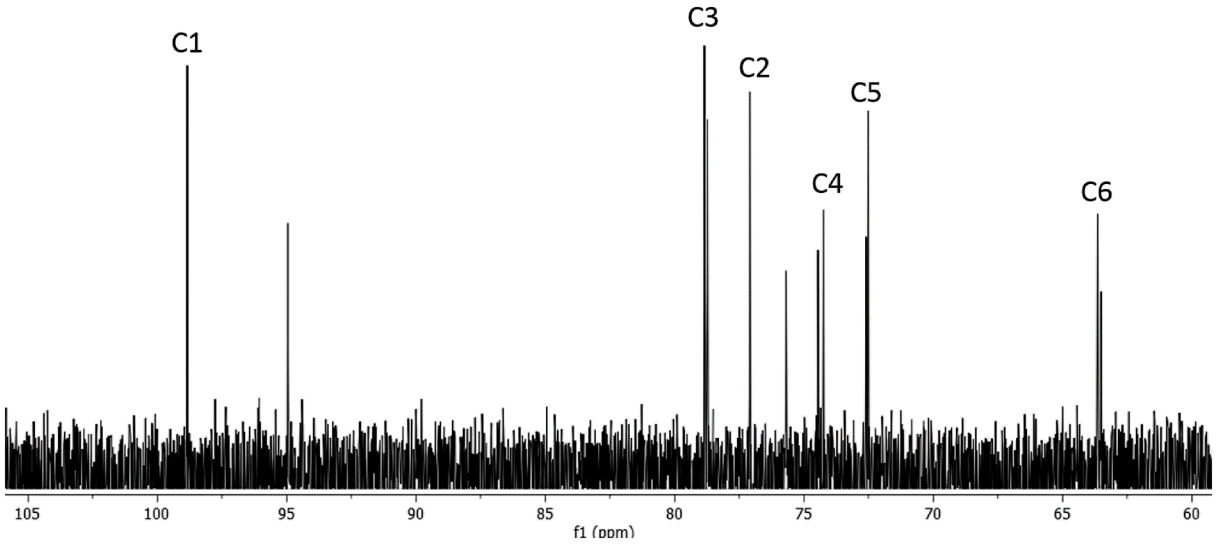

Fig. 6. ^{13}C NMR spectra of (1–3)-β-D-glucan of *Lignosus rhinocerus* strain ABI.

generate the mycelial biomass, which was used for the extraction of (1,3)-β-D-glucan (G), subsequent spectrophotometrical characterization using Fourier-Transform Infrared Spectroscopy (FT-IR) and one-dimensional (1D) and two-dimensional (2D) nuclear magnetic resonance (NMR), and elucidation of the structural aspects of the isolated materials. The biological activity of the G compound was also evaluated for its antioxidant properties. To our knowledge, this study is the first to report a characterized glucan from the mycelium of *L. rhinocerus* originating from a cultured bioreactor.

2. Materials and methods

2.1. Material

The tiger milk mushroom sample was obtained from a tropical forest in Lata Iskandar on July 7, 2018 (4.3244° N, 101.3249° E), Pahang, Malaysia (Fig. 1). The wild mushroom was transported to the Bioreactor and Propagation Lab, Agro-Biotechnology Institute (ABI), Serdang, Malaysia for further analysis. Upon arrival from the site, the sclerotium was cultured on potato dextrose agar (PDA) media plates to assure viability and prevent contamination. The plates were subsequently incubated under dark conditions at 30 °C for 10 days and then

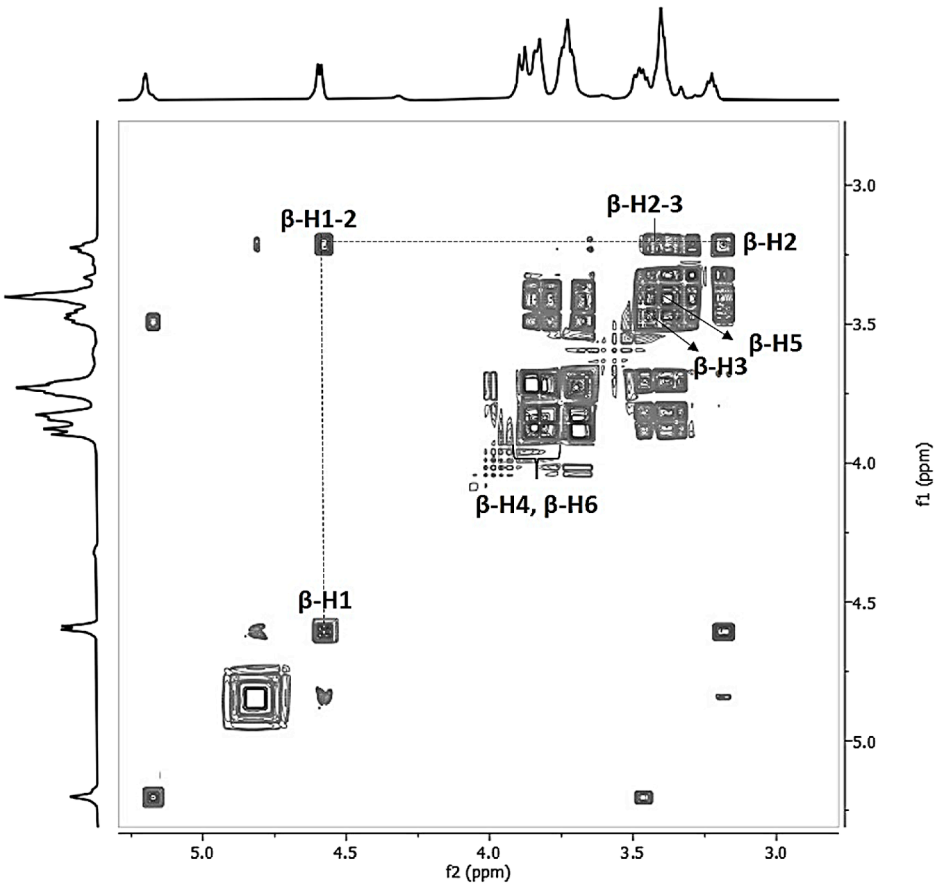

Fig. 7. $^{1}H/^{1}H$ COSY correlation of mycelial (1, 3)-β-D glucan of *Lignosus rhinocerus* strain ABI.

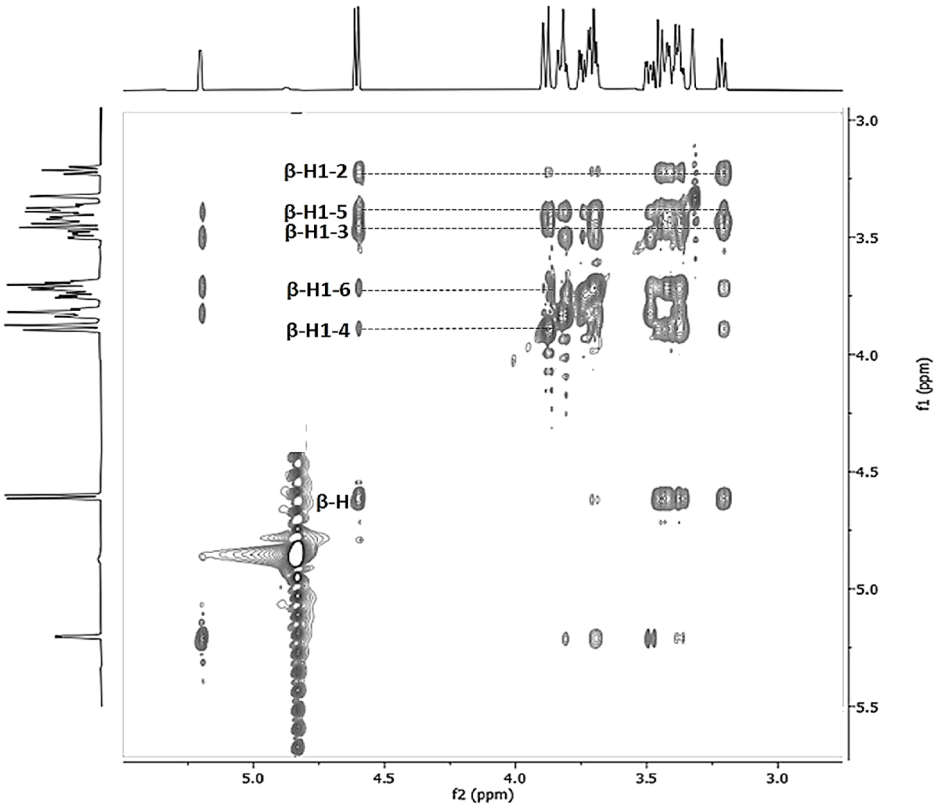

Fig. 8. $^{1}H/^{1}H$ TOCSY correlation spectrum for a spectrum of mycelial (1, 3)-β-D glucan of *Lignosus rhinocerus* strain ABI.

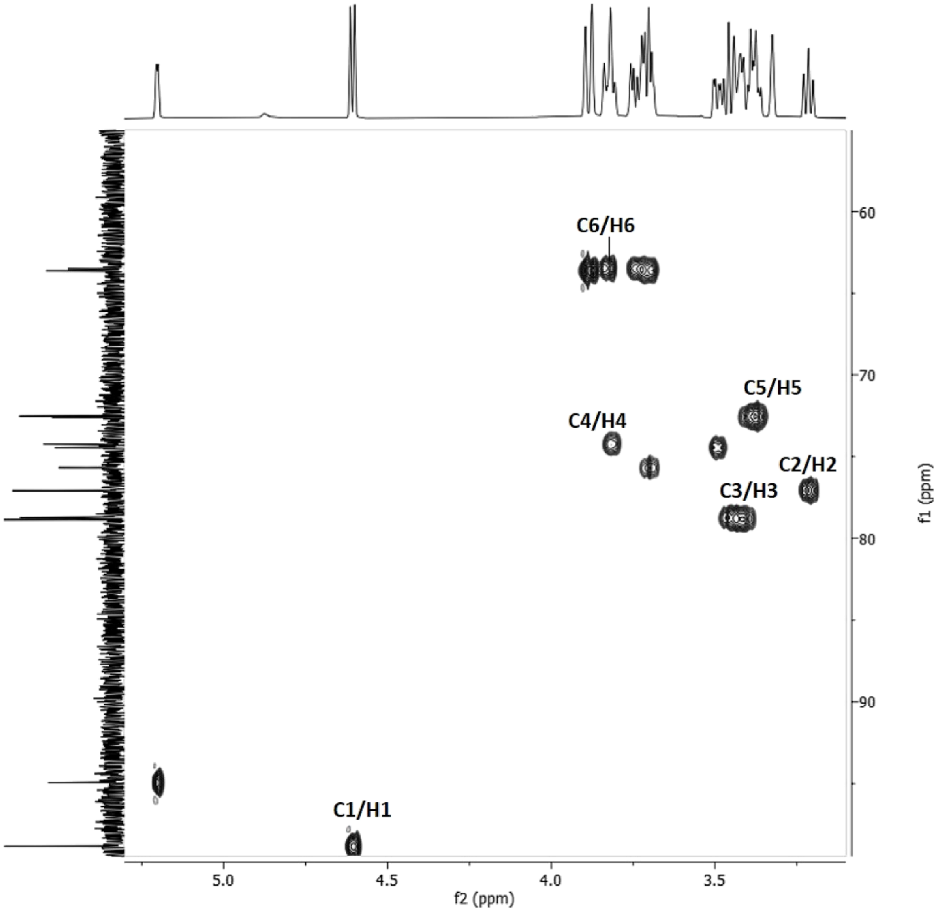

Fig. 9. $^{1}H/^{13}C$ HMQC correlation of mycelial (1, 3)-β-D glucan of *Lignosus rhinocerus* strain ABI.

maintained at 4 °C (Wan-Mohtar et al., 2016a). The strain was stored on PDA slants for preservation purposes.

2.2. Fungal isolation and phylogenetic tree analysis

2.2.1. DNA extraction of mycelium

Fungal DNA extraction was carried out using an improvised method (Liu et al., 2000). The mycelia of tiger milk mushroom (*L. rhinocerus* strain ABI) sample cultured on PDA plates was transferred aseptically using a sterile toothpick into lysis buffer (500 µL) in 1.5 mL Eppendorf tube [60 mM EDTA [pH 8.0], 400 mM Tris-HCl (pH 8.0), 150 mM NaCl, and 1% sodium dodecyl sulphate]. The tubes were then placed at room temperature for 10 min, after which 150 µL of potassium acetate (60 mL of 5 M potassium acetate, 11.5 mL of glacial acetic acid, and 28.5 mL of distilled water, pH 4.8) was added and the samples were mixed briefly by vortexing and then centrifuged at 11,000×*g* for 60 s. The supernatant was transferred into a new 1.5 mL Eppendorf tube, followed by adding isopropyl alcohol in a 1:1 ratio and the sample was mixed by inversion. The tube was centrifuged at 10,000×*g* for 120 s, the supernatant was removed, and 70% ethanol (300 µL) was used to wash the DNA pellet before it was centrifuged again at 10,000×*g* for 60 s. The supernatant was removed, and the resulting DNA pellet was air-dried.

2.2.2. PCR amplification

The resulting DNA pellet was dissolved in 1X Tris-EDTA (50 µL) to form a purified fungal gDNA. For fungal identification, two internal transcribed spacer (ITS) primers, which were ITS1: 5′-TCCGTAGGTGAACCTGCGG-3′ and ITS4: 5′-TCCTCCGCTTATTTGATATGC-3′, were used for the PCR. The modified PCR procedure of Liu et al. (2000) and Tamura et al. (2013) was followed using 25 µL of reaction mixture. The PCR mixture included 0.5 pmol of both primers, 0.5 U DNA polymerase (Promega, Madison, USA), 200 µM of dNTP mix (Promega), PCR buffer (ThermoFisher Scientific, Waltham, USA), and water. The targeted fragments were amplified using an Eppendorf Mastercycler gradient (Eppendorf, Hamburg, Germany) with the following procedure: 98 °C for 120 s; 25 cycles of 98 °C for 15 s, 60 °C for 30 s, 72 °C for 30 s, and 72 °C for 10 min for the final extension.

2.2.3. Data analysis

The resultant PCR products were separated on an agarose gel (1%) at 80 V for 1 h. The PCR products purified using a PCR Purification Kit (Tiangen Biotech Co., China) and BigDye® Terminator v3.1 Cycle Sequencing Kit (Applied Biosystems Co., USA) for bidirectional sequencing. BLAST analysis was performed against sequences from the same or different species and matched to the 10 closest species in the database.

2.2.4. Phylogenetic tree and species verification

A phylogenetic tree diagram was established according to the method described by Ab Kadir et al. (2016). Evolutionary distance (K_{nuc}) among sequences of the same fungal species was calculated using the neighbour-joining (NJ) method with MEGA software version X (Tamura et al., 2013). The closest K_{nuc} of the isolated commercial fungus was classified as the same species. To verify the species, sequence of the closest K_{nuc} species and the sequence of gDNA were compared for mismatches using A plasmid Editor (ApE) software. The results acquired were submitted to GenBank and analysed via BLAST search (http://blast.ncbi.nlm.nih.gov/) on the GenBank database.

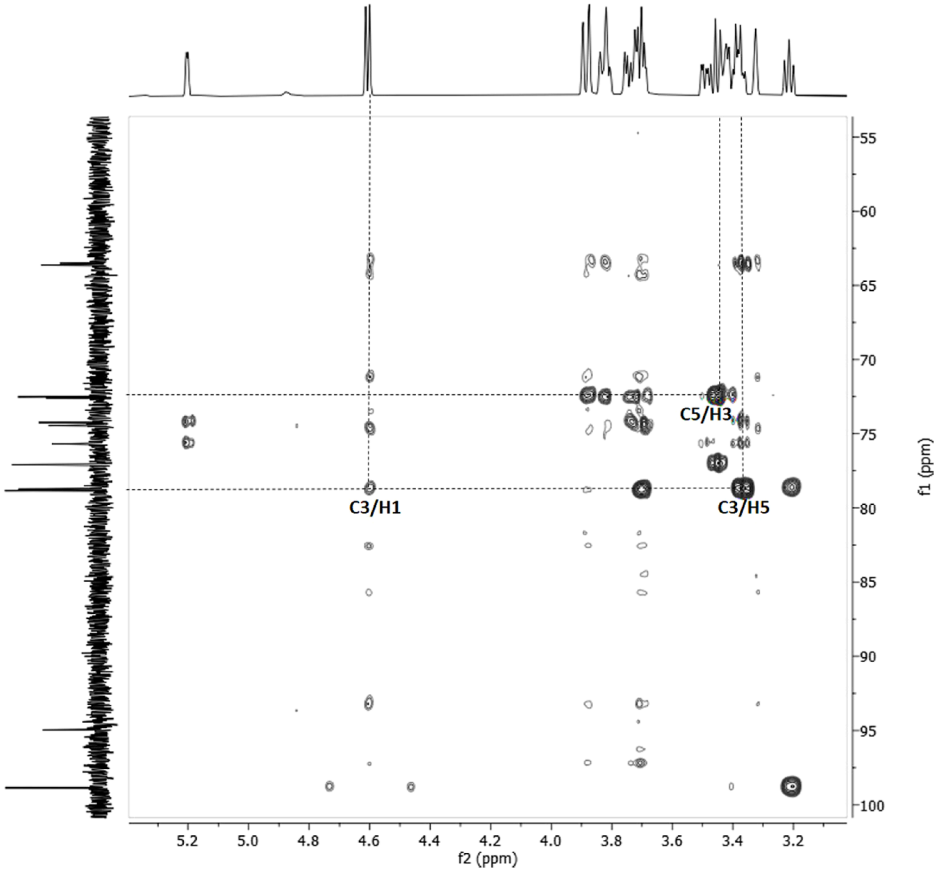

Fig. 10. $^{1}H/^{13}C$ HMBC correlation of mycelial (1, 3)-β-D glucan of *Lignosus rhinocerus* strain ABI.

2.3. Batch fermentation

A seed culture for batch fermentation was prepared in a baffled shake flask. First, two mycelia agar squares (1 cm × 1 cm) were cut from the culture plate using a sterile scalpel in a laminar flow chamber and inoculated into 100 mL medium consisted of 4% (w/v) of glucose, 0.1% (w/v) of yeast extract, 0.2% (w/v) of peptone, 0.046% (w/v) of potassium dihydrogen phosphate (KH_2PO_4), 0.1% (w/v) of dipotassium hydrogen orthophosphate (K_2HPO_4), and 0.05% (w/v) of magnesium sulphate ($MgSO_4$). Flasks were placed on a rotary incubator shaker at 30 °C, 200 rpm speed for 11 days with an initial pH of 5.5.

The fermentation was performed in a 10 L stirred-tank bioreactor (STR) (Labfors, Infors H-T, Switzerland). The seed culture (10% v/v) was inoculated into the medium. The media composition was similar to the shake flask media. The fermentation parameters were temperature (30 °C), aeration rate (1 vvm), agitation speed (200 rpm), dissolved oxygen (30%–40%), and initial pH (5.5). The mycelium was cultured in the bioreactor for 14 days and the resulting mycelial pellets were isolated.

2.4. Analytical methods

2.4.1. Extraction of crude (1,3)-β-D-glucan (G)

The exopolysaccharide-derived β-glucan (G) was extracted according to the protocol of Supramani et al. (2019a). The mycelia were filtered from the fermented culture broth and rinsed with distilled water. The filtrate obtained was added to 95% (v/v) ethanol at a ratio of 1:4 (g/mL) and left overnight at 4 °C for the precipitation of macromolecules. The sample was then centrifuged at 10,000 rpm for 15 min. The supernatant was discarded, and the pellet was drying in a food dehydrator at 35 °C until constant weight. The dried brown powder obtained was kept at room temperature for further analysis.

2.4.2. Measurement of β-D-glucan content

The level of β-D-glucan in the sample was measured using a Megazyme kit (Cat. no. K-YBGL) according to the manufacturer's protocol. The kit was used to evaluate enzymatic hydrolysis for measurement of total glucan and acid hydrolysis for α-glucan. Approximately 100 mg of sample was used to determine the total glucan (including α-glucan, β-glucan, D-glucose in oligosaccharide, sucrose and free D-glucose).

Next, for the α-glucan (including phytoglycogen, starch, D-glucose in sucrose and free D-glucose) determination, another 100 mg of sample was re-run accordingly. For glucose content analysis for both total and α-glucan; 0.1 mL of the supernatant was incubated with 3.0 mL of GOPOD reagent at 40 °C for 20 min. The D-glucose solution was used as standard (1 mg/mL) and the acetate buffer (200 mM, pH 5) as reagent blank, both were also incubated with GOPOD reagent. The glucose content analysis was carried out using UV–Visible spectrophotometer (Varian, Cary 50, USA) and the absorbance was measure at 510 nm. Finally, the β-glucan content [unit: g/100 g dry weight (DW)] was calculated by subtracting the percentage of total glucan and α-glucan by using Equation (1) as follows:

$$\%\beta - \mathrm{D} - \mathrm{glucan} = \frac{Total\ glucan - \alpha - D - glucan}{Total\ glucan} \times 100\% \quad (1)$$

Table 1
Chemical shifts (ppm) of ^{1}H and ^{13}C NMR signals for G recorded in D_2O at 25 °C.

Sugar residue	H1/C1	H2/C2	H3/C3	H4/C4	H5/C5	H6/C6	H6′
(1 → 3)-β-D-glucan	4.60 98.80	3.23 77.09	3.47 78.85	3.92 74.46	3.37 72.52	3.89 63.64	3.69

2.5. Structural characterization

2.5.1. Infrared spectroscopy

An FT-IR spectrum of the G sample (5 mg) was taken using Agilent Cary 630 equipped with diamond ATR (Attenuated Total Reflectance) FT-IR spectrophotometer (Agilent Cary 630 equipped with diamond ATR). The wavelength was recorded in the range of 4000–650 cm^{-1} and analysed using a real-time Micro-Lab software.

2.5.2. NMR spectroscopy

The spectra of 1D NMR (^{1}H and ^{13}C), and 2D NMR (correlation spectroscopy (COSY), total correlation spectroscopy (TOCSY), Heteronuclear Multiple-Quantum Coherence (HMQC) and Heteronuclear Multiple Bond Correlation (HMBC)) experiments were performed using 600-MHz NMR spectrometer (Agilent, USA). The G sample (10 mg) was mixed with 0.375 mL of tetradeuteromethanol (CD_3OD) and 0.375 mL buffer in D_2O (pH 6.0) containing TSP [0.1% (w/w)] in a 1.5-mL Eppendorf tube. The sample was vortexed for 60 s and sonicated at room temperature for 20 min before centrifuged at 10,000 × *g* for 10 min to obtain a clear supernatant. The supernatant (600 μL) was transferred to an NMR tube (5 mm, Norell, Sigma Aldrich, Canada) for NMR analysis. The comparison standard for ^{1}H NMR used for G was laminarin (*Laminaria digitata*, Sigma-Aldrich, Dorset, UK) and performed at 80 °C to generate a better separation of spectra. While all other experiments for G were conducted at 25 °C. A presaturation pulse sequence (PRESAT) experiment was performed to remove the large signal for the HOD to determine ^{1}H NMR spectra.

2.6. Antioxidant activity

2.6.1. Total phenolic content (TPC)

Total phenolics content (TPC) of the exopolysaccharide was determined by using Folin-Ciocalteou (F–C) (R & M Chemicals, UK.) reagent method with slight modifications (Sulaiman and Ooi, 2012). 10 μl of exopolysaccharide was diluted in distilled water (50 mg/mL) and mixed with 25 μl of fresh F–C reagent in the well of 96-well plate. After 5 min, the solution was mixed with 25 μl of 20% sodium bicarbonate (Na_2CO_3) (R & M Chemicals, UK) solution and left for 30 min at room temperature. Absorbance was read at 760 nm with microplate reader (Thermo Scientific Multiskan GO, Vantaa, Finland). The TPC of each extract was calculated by comparing the absorbance with the gallic acid calibration curve (0–1 mg/mL) according to Equation (2):

$$TPC = CV/g \tag{2}$$

where, C is concentration of the gallic acid equivalent from standard curve (mg/ml); V is volume of the extract (ml) and g is weight of extract (g). The contents were expressed as Gallic acid equivalent (mg GAE/g).

2.6.2. Ferric reducing antioxidant power (FRAP)

The FRAP assay was modified from the method of Sulaiman and Ooi (2012). FRAP reagent was freshly prepared by mixing 300 mM acetate buffer pH 3.6, 10 mM TPTZ in 40 mM HCl, and 20 mM FeCl3·6H2O in a volume ratio of 10:1:1 (v/v), respectively. To determine FRAP activity, 20 μl of EPS (50 mg/mL) was diluted in distilled water, mixed with 180 μl of FRAP reagent wells of a 96-well plate, and incubated for 30 min at room temperature in the dark. Absorbance was measured at 593 nm using a plate reader (Thermo Scientific Multiskan GO, Vantaa, Finland). Ferrous sulphate ($FeSO_4$) solution (0.1, 0.2, 0.4, and 0.6 mM) was used as the standard and FRAP activity was calculated as ferrous equivalent (mM FE (II)/mg). Ascorbic acid was used as a positive control.

2.6.3. 2, 2-diphenyl-1-picrylhydrazyl (DPPH)

The DPPH free radical scavenging activity assay was carried out according to the method described by Sulaiman and Ooi (2012) with slight modification. EPS (50 μl) was diluted in distilled water (0–50.0 mg/mL) and mixed with 150 μl of 0.3 mM DPPH solution in methanol in the wells of a 96-well plate. The plate was kept in the dark for 30 min before absorbance of the solution was measured at 517 nm. Ascorbic acid was used as a positive control. Antioxidant activity was determined over a range of concentrations to establish IC50 (the concentration that reduced DPPH absorbance by 50%). Percentage inhibition of the DPPH scavenging effect was calculated according to equation (3):

$$\text{DPPH inhibition}\,(\%) = \frac{\Delta A517\ of\ control - \Delta A517\ of\ sample}{\Delta A517\ of\ control} \times 100 \tag{3}$$

2.7. Statistical analysis

All experiments were performed in triplicate, and the corresponding mean ± standard deviation (SD) was calculated using GraphPad Prism 5 software, version 5.0, and indicated as error bars. Error bars smaller than the symbol or icon size, do not appear in the figures.

3. Results and discussion

3.1. Morphological characteristics of an identified tiger milk mushroom

The different morphological stages of identified wild tiger milk mushroom *L. rhinocerus* strain ABI (LRSA) are shown in Fig. 1. The diagram illustrates the basidiocarp of LRSA found in Lata Iskandar, Malaysia with its underground sclerotium (Fig. 1A). Morphologically, *L. rhinocerus* can be distinctively characterized by its woody and hard appearance with an umbrella-shaped stipitate basidiocarp in the centre, emerging from a sclerotium. The pileus is concentrically zonate with an asymmetrical shape, glabrous, and tea-brown in colour. The shape of the identified LRSA resembles *L. tigris* and *L. cameronensis* (Tan et al., 2013). However, *L. rhinocerus* has a smaller pore size (6–8 per mm) compared with *L. tigris* (0.5–1 per mm) and *L. cameronensis* (2–3 per mm) (Fung and Tan, 2019). Furthermore, common *L. rhinocerus* has larger and distinctly broader ellipsoid basidiospores compared with *L. tigris* and *L. cameronensis* (Yap et al., 2013).

The pileus and stipe of *L. rhinocerus* are woody in form while the sclerotium is a hard, dense resting body, consisting of a compact aggregated hyphal mass (Georgiou et al., 2006). The sclerotia are asexual, multicellular, specialised reproductive features holding food reserve materials for mushroom sustenance in unsuitable growth conditions (Cheung, 2013). The sclerotia have an irregular spherical shape of about 4–5 cm in diameter (Abdullah et al., 2013). The surface of the sclerotium is rough and wrinkly and white to pale brown in colour (Fig. 1B). The internal structure is white and powdery (Fig. 1C), which is in agreement with Abdullah et al. (2013).

Mycelia differ significantly from fruiting bodies. When the sclerotia of *L. rhinocerus* were cultured on PDA media, the mycelium texture appeared furry and cottony with a colony colour of white to beige or light yellow, as shown in Fig. 1D. As described by Yap et al. (2014), the expansion of the germ tube of mycelium eventually develops into a ring or spherical shape, referred to as “tiger eyes” (Fig. 1D). Mobilization of the growing mycelium enables nutrient uptake through cross-linking of the expanding hyphae. Tiger milk mushroom can be

Table 2
Antioxidant properties of G.

Concentration of G	TPC	FRAP	DPPH
	Gallic Acid (mg GAE/g)	Ferrous sulphate (mM Fe(II)/g)	IC50 (mg/ml)
	1 g/mL	50 mg/mL	0–50 mg/mL
L. rhinocerus strain ABI	4.47 ± 0.06	0.56 ± 0.02	11.48 ± 0.50
Ascorbic acid (0–0.1 mg/mL)	–	0.18 ± 0.01	0.022 ± 0.002

cultured on other types of agar media, where it presents a similar appearance to that when grown on PDA media (Abdullah et al., 2013). However, under liquid cultivation, the mycelia grow in a stable pellet structure form as illustrated in Fig. 1E.

3.2. Molecular characteristics of identified tiger milk mushroom

In the present study, LRSA was selected for the construction of a phylogenetic tree and biomolecular identification. Thus, the DNA of LRSA was extracted and PCR was performed to amplify the partial region of LRSA rDNA using ITS1 and ITS4 primers. As a result, an amplified PCR product of rRNA of approximately 515 bp in size was obtained as shown in Fig. 2. NCBI BLAST analysis was used to sequence and align the product with the top 9 related species, with 14 Ganoderma species as the outgroup. The *L. rhinocerus* strain ABI sequence was found to be 99% similar to (FJ899143.1) *L. rhinocerus* strain CH31 and (FJ3380871.1) *L. rhinocerus* strain CH2 located at clade A (Fig. 3). Subsequently, the evolutionary distance (K_{nuc}) was calculated between sequences of similar fungus species using MEGA software version X for further investigation. A phylogenetic tree was constructed using the neighbour-joining (NJ) method from K_{nuc} data using the same software. The closest evolutionary distance K_{nuc} values indicated that the fungal isolate was closely related to *L. rhinocerus* (K_{nuc} 0.003) at clade A. The fungal species was verified by using a plasmid matching software (ApE) in which the isolated fungal was found to belong to the *L. rhinocerus* species (see the supplementary data Fig. S1), which aligned with *L. rhinocerus* strain CH2 and *L. rhinocerus* strain CH31 sequences.

3.3. β-D-glucan content

In the present study, approximately 100 mg of sample was used to determine the total glucan (including α-glucan, β-glucan, D-glucose in oligosaccharide, sucrose and free D-glucose). The results for total glucan, α-glucan, and β-D-glucan or D-glucose content from the mycelium of *Lignosus rhinocerus* were 40.49 ± 5.7% (w/w), 4.19 ± 2.6% (w/w) and 36.3 ± 1.50% (w/w), respectively. Other polysaccharide monomers (63.7%, calculated by difference) identified in fungal EPS would potentially be hexoses (glucose, mannose, galactose, fucose, rhamnose, talose) but also pentoses (arabinose, ribose, xylose) (Jaros et al., 2018; Kim et al., 2000). As the structure is polysaccharide-protein complex, 59.51% would be the protein structure that holds the polysaccharide. In our research, antioxidative D-glucose or D-glucan was the key active compound which specifically related to its antioxidative strength. According to Mcleary and Draga (2016), medicinal mushrooms key active components were identified as 1,3:1,6-β-glucan, triterpenoids and ergosterol.

From this result, it appeared that β-D-glucan represented almost 90% of the total glucan content of the aqueous extracts of mycelium of LRSA and mostly composed of D-glucose as compared with the standard. It was reported by McCleary and Draga (2016) that major structural feature of mushroom species consists of (1,3)-β-glucan backbone with D-glucose as the monosaccharide. Previous studies on sclerotia of *Lignosus rhinocerotis* (Cooke) Ryvarden (synonym: *Lignosus rhinocerus*) verified the polysaccharide extracted from the tuber consists of polysaccharide-protein complex and a glucan with glucose content of 98.6% (Lai et al., 2008). In addition, Lau et al. (2013a,b) also reported that 82–93% of total glucans of tuber *L. rhinocerus* were β-D-glucan which composed of majority of D-glucose. Together, our mycelial-based glucan showed close comparability with tuber-based glucan.

3.4. IR spectroscopy

FT-IR spectroscopy is a valuable technique for the structural characterization of exopolysaccharides (Prado et al., 2005) and can be used to analyse fungal glucans from various mushroom and fungal sources due to its sensitivity to the position and anomeric configuration of glycosidic linkages in glucans (Synytsya and Novak, 2014).

The FT-IR spectrum of compound G is presented in Fig. 4B. By comparison with laminarin (Fig. 4A), the broad and intense absorption peak at 3277 cm^{-1} was found to represent the stretching vibration of a hydroxyl group (O–H), which indicated the presence of a polyhydroxilic compound (Liu et al., 2007). The absorption peak at 2919 cm^{-1} was assigned to the stretching vibration of C–H bonds, indicating a methylene group (CH_2) (Paulo et al., 2012). The spectra also showed adsorbed water bending vibration at 1638 cm^{-1} (Miao et al., 2014). Other major absorption bands identified at 1545 cm^{-1} and 1400 cm^{-1} were attributed to amide group and -CH3 stretching vibration, respectively (Ji et al., 2013). The absorption band at approximately 1078 cm^{-1} can be assigned to C–O stretching vibration and a pyranose ring (C–O–C) (Hu et al., 2017). The absorption peaks responsible for O–H, C–H, and C–O groups were characteristic of the FT-IR absorption of polysaccharide (Wang and Zhang, 2009). The 'fingerprint' region for carbohydrates in the range of 850–1000 cm^{-1} can be used to determine polysaccharide type and configuration (Hu et al., 2017). Thus, the specific absorption peak at 896 cm^{-1} corresponding to the presence of β-configuration in the 'anomeric region', indicating that the compound G contained β-type glycosidic linkages (Wan-Mohtar et al., 2016b).

3.5. NMR spectroscopy

3.5.1. 1D NMR (^1H and ^{13}C) analysis

The structure of G was further elucidated using NMR spectral analysis. Fig. 5 shows the ^1H NMR spectra using D_2O as a solvent. ^1H NMR spectra profiling presents a broad fingerprint of a biomolecule in solution (Pomin, 2012). Generally, for D-glucose or D-glucan analysis, the anomeric region appears at the most downfield region of the spectra, which is usually located between 4.0-6.0 ppm (Fig. 5) with most of the β-anomeric protons appear in the range of 4.0–5.0 ppm while most of the α-anomeric protons appear in the range of 5.0–6.0 ppm (Hu et al., 2016). In the ^1H NMR spectra of our exopolysaccharide LRSA (Fig. 5), a signal at 5.20 ppm with the coupling constant (*J*) of 3.73 Hz indicated the H1-α anomer. Another peak at 4.60 ppm exhibited a significantly larger *J* value (7.93 Hz) as expected for the H1-β anomer, which appeared upfield from the hydrogen of the α anomer. Another obvious signals was at 3.23 ppm, indicating the H2-β anomer (Gurst, 1991). The ^1H NMR spectra of LRSA had a similar pattern to the spectra obtained in previous studies for glucopyranose (Glcp), after achieving anomeric equilibrium in solution (Pomin, 2012). At equilibrium, the percentage of each anomer of D-glucopyranose was 64% for the β-anomer and 36% for the α anomer, with the β-D-glucopyranose reported to be the more stable anomer (Gurst, 1991). This finding was comparable with previous study by Ji et al. (2013) which analysed laminarin in the area of ^1H NMR spectrum of δ 4.49–5.5 ppm. Besides, it was also comparable with its closest counterpart genus *Lignosus rhinocerotis* sclerotia (Hu et al., 2017) β-D-glucan with

Table 3
Comparison of characterized tiger milk mushroom mycelial glucan with the literature.

Organism name	Geographical Origin	DNA source	Fungal size	Polysaccharide linkages	Total cultivation time (day)	β-glucan content (w/w) %	FT-IR (wavelength, cm^{-1})	^1H NMR	Reference
L. rhinocerus strain ABI	Lata Iskandar, Malaysia	Mycelium (Liquid fermentation)	515 bp	(1,3)-β-D-glucan	25	36.3	3277, 2919, 1638, 1545, 1400, 1078, 896	OH-2, OH-4, OH-6	*Current work*
L.rhinocerus	Lata Iskandar, Malaysia	Sclerotium (cultivated)	NA	β-D-glucan	132	63.51	NA	NA	Jamil et al. (2018)
L. tigris	Selangor, Malaysia	Sclerotium (cultivated)	NA	β- glucans	180	5.85–16.74	NA	NA	Kong et al. (2016)
L. rhinocerotis strain TM02	Selangor, Malaysia	Sclerotium (cultivated)	NA	β- glucans	180	1.1 and 3.2	NA	NA	Lee et al. (2014)
Lignosus spp. strain M26/08, M49/07, M23/08	Kuala Lumpur, Semenyih & Kuala Lipis, Malaysia.	Sclerotium (wild)	NA	β-D- glucans	NA	NA	1680, 1657, 1639, 1620, 1471	NA	Choong et al. (2014)
L. rhinocerotis	Negeri Sembilan, Malaysia	Fruit body (cultivated), Sclerotium (cultivated), Mycelium (Liquid fermentation)	NA	(1,3) and (1,6) - β-D- glucans	111	9.3 to 13.2	NA	NA	Lau et al. (2013a)
L. rhinocerotis	Negeri Sembilan, Malaysia	Sclerotium (cultivated)	NA	(1,3)-β- and (1,6)-β glucans	111	38.93	NA	NA	Lau et al. (2013b)
L. rhinocerus	Pahang, Malaysia	Fruit body (wild)	NA	(1,3) and (1,6) - β-D- glucans	NA	33.9	NA	NA	Jamil et al. (2013)

*NA = not available. TMM = Tiger Milk mushroom. Bp = Base pair.

our *Lignosus rhinocerus* mycelium showing also β-D-glucan. Evaluation of the 'anomeric region' of ^1H NMR spectra in this study with those described previously specifies that they are of similar pattern (Hu et al., 2017; Kim et al., 2000; Liu et al., 2014; Wagner et al., 2003). Thus, these spectra indicate that the glycosidic bonds in glucan (Fig. 5) was β-type. In addition, in the ^1H NMR spectra of compound G of LRSA, the chemical shifts at 4.6, 3.9, and 3.8 ppm were attributed to the hydroxyl groups OH-2, OH-4, and OH-6, respectively (Supramani et al., 2019b; Wagner et al., 2003).

Multiple compressed, overlapping, and unresolved proton signals in the ^1H NMR spectra mean that the application of other nuclei such as ^{13}C is important for the characterization of polysaccharides. Fig. 6 illustrates the ^{13}C NMR spectrum obtained for G compound of LRSA. It can be observed that the pattern obtained for ^{13}C NMR from this study has similar pattern to the 13C NMR achieved for D-glucose with anomeric region is between 90-110 ppm and the β-anomer appeared the most downfield in the spectra (Brown et al., 2018; Gurst, 1991; Kim et al., 2000; Pomin, 2012). This indicated that glucan has β-configuration of D-glucosyl residues at peak 98.80 ppm for C1 (Fig. 6). Hence, the ^{13}C spectrum (Fig. 6) clearly revealed the shifts in carbons (C1–C6) characteristic of a β-glucan: 98.8 ppm (C1), 77.1 ppm (C2), 78.8 ppm (C3), 74.2 ppm (C4), 72.5 ppm (C5), and 63.6 ppm (C6), in agreement with previous studies (Gonzaga et al., 2013; Liu et al., 2014; Pomin, 2012). According to Emwas et al. (2018), the quality of spectra and their subsequent interpretation in NMR are influenced by multiple factors such as sample characteristics, NMR setup, and processing parameters. In the present study, the ^{13}C NMR spectrum of G showed that the chemical shifts of C1 and C3 had moved downfield compared with those of glucose, indicating that the glycosidic bond in G was of the β-(1 → 3) type, which was in agreement with Ji et al. (2013).

3.5.2. 2D NMR (COSY, TOCSY, HMQC & HMBC) structural analysis

Two-dimensional (2D) NMR spectra were used to confirm the attributions recorded by ^1H and ^{13}C in 1D NMR spectra to reveal the characteristics of the exopolysaccharide. 2D NMR is a powerful tool for structure elucidation, and has been shown to provide conclusive evidence for β-(1,3) linkages (Ensley et al., 1994; Lowman et al., 2011). Although many studies have used methylation analysis to determine the glycosidic linkages of β-glucans, this approach is more time-consuming and requires careful pre-treatment and interpretation of the generated data (Hakamori, 1964; Sims et al., 2018).

Fig. 7 and Fig. 8 show the bidimensional COSY and TOCSY spectra with identification of the couplings between the protons ($^1H/^1H$). Based on COSY and TOCSY spectra analysis, all ^1H-chemical shifts can be fully identified and assigned accordingly for the 1D ^1H NMR spectrum in alignment with previous studies (Gonzaga et al., 2013; Nie et al., 2011). Fig. 9 represents the NMR spectra for HMQC, with a record of the couplings between carbons and hydrogens of the glycosidic ring ($^{13}C/^1H$). Using a carbon-related experiment for the HMQC spectrum, all ^1H-linked carbons signals can also be assigned through correlation with one-bonded ^1H–^{13}C *J*-couplings. The HMQC spectrum (Fig. 9) revealed the spectrum of distinct cross peaks in the anomeric region of G. The C1, C2, C3, C4, C5, and C6 signals at 98.8, 77.1, 78.8, 74.2, 72.5, and 63.6 ppm cross-link to the proton signals H1, H2, H3, H4, H5, and H6 at chemical shifts 4.60, 3.23, 3.47, 3.92, 3.37, and 3.89 ppm, respectively, confirming the results obtained in 1D NMR. These values are fully consistent with the literature (Liu et al., 2014; Nie et al., 2011; Pomin, 2012). HMBC ($^1H/^{13}C$) provides correlations between protons and carbons that are separated from each other by two or three bonds or up to five-bond correlations (Vasavi et al., 2011). The linkage sequence of the adjacent glycosyl residues were deduced by the cross-peaks in the HMBC spectrum (Fig. 10). The cross-peak between H1 (4.60 ppm) and C3 (78.8 ppm) and between H5 (3.37 ppm) and C3 (78.8 ppm) indicated that residue was linked to residue G via a β-(1 → 3)-linked glycosidic bond (Wu et al., 2019). Finally, by compiling the information from 1D and 2D NMR, a complete assignment of all linkage patterns was obtained, as shown in Table 1. With the results of 2D NMR, the mycelial of LRSA was confirmed to consist of (1,3)-β-D-glucan linkages.

3.6. Antioxidant activity

The antioxidant properties of G were accessed using three antioxidant assays (Table 2): TPC, FRAP, and DPPH assays. Phenols are important plant constituents because of their scavenging ability, attributable to their hydroxyl groups. In the present study, total phenolic content was determined to investigate whether the antioxidant activities of G implicated its phenolic compounds. TPC of the 1 g/mL of exopolysaccharide contained 4.47 ± 0.06 mg GAE/g, a level slightly lower than that of previously reported studies (Lau et al., 2014). How-

ever, the concentration of total phenols in medicinal mushrooms has been reported as ranging between 4.45 mg GAE/g and 14.44 mg GAE/g (Abugri and Mcelhenney, 2013). Thus, the antioxidant capacity of G was determined to be within the expected range and may be related to the presence of phenolic compounds (Wan-Mohtar et al., 2018).

The reducing potential (reduction of Fe^{3+} to the Fe^{2+}) of exopolysaccharide was determined by FRAP assay. The reducing power for the 50 mg/mL of extract was 0.56 ± 0.02 mM Fe(II)/g, which was higher than that of *L. rhinocerus* (wild type) and *L. rhinocerus* TM02 (0.006–0.016 mM Fe(II)/g) (Yap et al., 2013). However, the reducing value was comparable to that of *L. rhinocerus* KUM61075 (0.21–0.85 mM Fe(II)/g) (Lau et al., 2014). In addition, the extract exhibited a relatively higher FRAP value in comparison with the positive control, the known antioxidant ascorbic acid (0.18 ± 0.01 mM Fe(II)/g). A higher FRAP value in extracts, regardless of their phenolic content, may indicate the existence of other less polar compounds such as tocopherols and flavonoids, which may possibly contribute to the reducing/electron-donating activities of the compounds (Yap et al., 2013).

The DPPH radical scavenging assay is a widely used method to evaluate antioxidant activities more rapidly compared with other methods. DPPH, a stable free radical, has a characteristic absorption at 517 nm. As antioxidants donate protons to these radicals, the absorption decreases. The decrease in absorption is taken as a measure of the extent of radical scavenging (Kalyoncu et al., 2010). Free radical scavenging values of G are shown in Table 2 as percentages. In the DPPH assay, the ability of G to reduce the stable DPPH radical into a non-radical form of DP was evaluated and IC_{50} of G was found to be 11.48 ± 0.50 mg/mL, indicating a higher free radical scavenging activity compared with previously reported studies of the antioxidant activities of *L. rhinocerus* (Lau et al., 2014; Yap et al., 2013). The extract showed higher radical scavenging activity than that of the positive control ascorbic acid (0.022 ± 0.002 mg/mL). These results indicate that the G compound of LRSA obtained in submerged cultivation may represent a valuable source of antioxidant compounds. Few studies to date have investigated the mycelium and broth culture and most all comparison studies have used sclerotia for investigation of bioactivities.

3.7. Comparison of characterized tiger milk mushroom glucan with the literature

The tiger milk mushroom mycelial glucan characterized in the present work was compared with that of previous studies, as shown in Table 3. The present study is the first comprehensive characterization of tiger milk mushroom in terms of strain determination using molecular identification, fungal PCR product size, sequence length, polysaccharide linkages, β-glucan content, FT-IR spectroscopy, and structural characterization using NMR. Six previous studies involving β-glucan studies have primarily considered the sclerotium of *L. rhinocerus* specifically originating from Malaysia (Choong et al., 2014; Jamil et al., 2013, 2018; Lau et al., 2013a, 2013b; Lee et al., 2014). However, the production of sclerotia using a solid-state fermentation technique requires a long cultivation period which is economically unfeasible and susceptible to contamination (Leskosek-Cukalovic et al., 2010). Few studies have used solid-state fermentation as sclerotia cultivation takes about 3–6 months (Jamil et al., 2018; Kong et al., 2016; Lau et al., 2013a; Lee et al., 2012), in contrast with the present study, in which the mycelium was produced in approximately 25 days. This motivated further investigation into the potential of the mycelium as an alternative to cultivated or wild sclerotia. The production of mycelium through submerged liquid fermentation has several advantages, including a shorter cultivation time, higher yields, and decreased contamination. Hence, a more efficient production of the desired products, particularly mycelial biomass and polysaccharides, can be obtained (Lau et al., 2014; Liu et al., 2014; Yang et al., 2013). The relevance of mycelium as a substitute for the sclerotia is supported by the current findings, in which the β-glucan content extracted from mycelium (36.3% w/w) was comparable with or higher than that obtained from sclerotia in previous studies (5.85%–38.93% w/w) (Choong et al., 2014; Jamil et al., 2013, 2018; Kong et al., 2016; Lau et al., 2013a, 2013b; Lee et al., 2014). This observation is also supported by the study of Lau et al. (2014), which reported that the mycelium of *L. rhinocerotis* had bio-activities comparable with those of the sclerotia, prompting further consideration of the mycelium as an alternative source of functional components. The current work also includes FT-IR spectroscopy analysis to investigate the exopolysaccharide linkages of the mycelium of *L. rhinocerus* in contrast to previous studies. (1,3)-β-D-glucan was identified as the main linkage in compound G and was extracted from a mycelium sample, unlike the work described by Choong et al. (2014) which investigated only the extent of β-D-glucan linkage in a sclerotia sample.

4. Conclusion

The Malaysian tiger milk mushroom *Lignosus rhinocerus strain* ABI (LRSA) was morphologically identified through biomolecular characterization. The structure of its bioactive compound, (1,3)-β-D-glucan (G) from the extracted mycelium cultured in a bioreactor, was successfully characterized and elucidated spectrophotometrically using FT-IR and NMR. NMR structural analysis in the present study represents the first structural characterization of (1,3)-β-D-glucan of *L. rhinocerus*. Furthermore, the evaluation of antioxidant activity showed that LRSA has effective antioxidant properties with high free radical scavenging activity.

Compliance with ethical standards

The written article complies with the ethical standards.

Declaration of competing interest

There is no conflict of interest for this journal article.

Acknowledgements

This work was supported by the University of Malaya under Fundamental Research Grant Scheme [FRGS: FP066-2018A] via Ministry of Education, Malaysia and Satu Joint Research Programme (ST006-2019) and Bio-Analytical Industry Development Programme (BIDP/1-2014(06)) award under Agro-Biotechnology Institute, Malaysia.

Appendix A. Supplementary data

Supplementary data to this article can be found online at https://doi.org/10.1016/j.bcab.2019.101455.

References

Ab Kadir, S., Wan-Mohtar, W.A.A.Q.I., Mohammad, R., Abdul Halim Lim, S., Mohammed, A.S., Saari, N., 2016. Evaluation of commercial soy sauce koji strains of *Aspergillus oryzae* for γ-aminobutyric acid (GABA) production. J. Ind. Microbiol. Biotechnol. 43, 1387–1395. https://doi.org/10.1007/s10295-016-1828-5.

Abdullah, N., Abdul, W.A.I., Beng, F.Y.E.L., Zainal, A.N., Aminudin, N., 2011. Anti-cervical cancer activity and SELDI-TOF-MS analysis of proteins from *Lignosus rhinocerus* (Tiger's Milk Mushroom) grown in stirred tank reactor. Pept. Sci. Proc. Japanese Pept. Symp. 78 2010.

Abdullah, N., Haimi, M.Z.D., Lau, B.F., Annuar, M.S.M., 2013. Domestication of a wild medicinal sclerotial mushroom, *Lignosus rhinocerotis* (Cooke) Ryvarden. Ind. Crops Prod. 47, 256–261. https://doi.org/10.1016/j.indcrop.2013.03.012.

Abugri, D.A., Mcelhenney, W.H., 2013. Extraction of total phenolic and flavonoids from edible wild and cultivated medicinal mushrooms as affected by different solvents. J. Nat. Prod. Plant Resour. 3, 37–42.

Bowman, S.M., Free, S.J., 2006. The structure and synthesis of the fungal cell wall.

Bioessays 28, 799–808. https://doi.org/10.1002/bies.20441.
Brewer, M.S., 2011. Natural antioxidants: sources, compounds, mechanisms of action, and potential applications. Compr. Rev. Food Sci. Food Saf. 10, 221–247. https://doi.org/10.1111/j.1541-4337.2011.00156.x.
Brown, G.D., Bauer, J., Osborn, H.M.I., Kuemmerle, R., 2018. A solution NMR approach to determine the chemical structures of carbohydrates using the hydroxyl groups as starting points. ACS Omega 3, 17957–17975. https://doi.org/10.1021/acsomega.8b02136.
Cheung, P.C.K., 2013. Mini-review on edible mushrooms as source of dietary fiber: preparation and health benefits. Food Sci. Hum. Wellness 2, 162–166. https://doi.org/10.1016/j.fshw.2013.08.001.
Choong, Y.K., Xu, C.H., Lan, J., Chen, X.D., Jamal, J.A., 2014. Identification of geographical origin of Lignosus samples using Fourier transform infrared and two-dimensional infrared correlation spectroscopy. J. Mol. Struct. 1069, 188–195. https://doi.org/10.1016/j.molstruc.2014.04.001.
Cui, B.K., Tang, L.P., Dai, Y.C., 2011. Morphological and molecular evidences for a new species of *Lignosus* (Polyporales, Basidiomycota) from tropical China. Mycol. Prog. 10, 267–271. https://doi.org/10.1007/s11557-010-0697-y.
Emwas, A.H., Saccenti, E., Gao, X., McKay, R.T., dos Santos, V.A.P.M., Roy, R., Wishart, D.S., 2018. Recommended strategies for spectral processing and post-processing of 1D 1 H-NMR data of biofluids with a particular focus on urine. Metabolomics 14, 1–23. https://doi.org/10.1007/s11306-018-1321-4.
Ensley, H.E., Tobias, B., Pretus, H.A., McNamee, R.B., Jones, E.L., William Browder, I., Williams, D.L., 1994. NMR spectral analysis of a water-insoluble (1 → 3)-β-d-glucan isolated from *Saccharomyces cerevisiae*. Carbohydr. Res. 258, 307–311. https://doi.org/10.1016/0008-6215(94)84098-9.
Fazenda, M.L., Seviour, R., McNeil, B., Harvey, L.M., 2008. Submerged culture fermentation of "higher fungi": the macrofungi. Adv. Appl. Microbiol. 63, 33–103. https://doi.org/10.1016/S0065-2164(07)00002-0.
Fung, S.-Y., Tan, C.-S., 2019. Tiger milk mushroom (the *Lignosus* trinity) in Malaysia: a medicinal treasure trove. Med. Mushrooms Recent Prog. Res. Dev. 349–369. https://doi.org/10.1007/978-981-13-6382-5_14.
Georgiou, C.D., Patsoukis, N., Papapostolou, I., Zervoudakis, G., 2006. Sclerotial metamorphosis in filamentous fungi is induced by oxidative stress. Integr. Comp. Biol. 46, 691–712. https://doi.org/10.1093/icb/icj034.
Gonzaga, M.L.C., Menezes, T.M.F., De Souza, J.R.R., Ricardo, N.M.P.S., Soares, S.D.A., 2013. Structural characterization of β glucans isolated from *Agaricus blazei* Murill using NMR and FTIR spectroscopy. Bioact. Carbohydrates Diet. Fibre 2, 152–156. https://doi.org/10.1016/j.bcdf.2013.10.005.
Gurst, J.E., 1991. NMR and the structure of d-glucose. J. Chem. Educ. 68, 1003–1004. https://doi.org/10.1021/ed068p1003.
Hakamori, S.-I., 1964. A rapid permethylation of glycolipid, and polysaccharide catalyzed by methylsulfinyl carbanion in dimethyl sulfoxide. J. Biochem. 55, 205–208. https://doi.org/10.1093/oxfordjournals.jbchem.a127869.
Hu, T., Huang, Q., Wong, K., Yang, H., Gan, J., Li, Y., 2017. A hyperbranched β-D-glucan with compact coil conformation from *Lignosus rhinocerotis* sclerotia. Food Chem. 225, 267–275. https://doi.org/10.1016/j.foodchem.2017.01.034.
Hu, T., Jiang, C., Huang, Q., Sun, F., 2016. A comb-like branched β-D-glucan produced by a *Cordyceps sinensis* fungus and its protective effect against cyclophosphamide-induced immunosuppression in mice. Carbohydr. Polym. 142, 259–267. https://doi.org/10.1016/j.carbpol.2016.01.036.
Jamil, N.A.M., Mohd Rashid, N.M.N., Hamid, M.H.A., Rahmad, N., Al-Obaidi, J.R., Yusoff, M.Y.M., Shaharuddin, N.S., Saleh, N.M., 2013. LCMS-QTOF determination of lentinan-like β-D-glucan content isolated by hot water and alkaline solution from tiger's milk mushroom, termite mushroom, and selected local market mushrooms. J. Mycol. 2013. https://doi.org/10.1155/2013/718963.
Jamil, N.A.M., Rashid, N.M.N., Hamid, M.H.A., Rahmad, N., Al-Obaidi, J.R., 2018. Comparative nutritional and mycochemical contents, biological activities and LC/MS screening of tuber from new recipe cultivation technique with wild type tuber of tiger's milk mushroom of species *Lignosus rhinocerus*. World J. Microbiol. Biotechnol. 34 (0). https://doi.org/10.1007/s11274-017-2385-4.
Jaros, D., Köbsch, J., Rohm, H., 2018. Exopolysaccharides from Basidiomycota: formation, isolation and techno-functional properties. Eng. Life Sci. 18, 743–752. https://doi.org/10.1002/elsc.201800117.
Ji, C.F., Ji, Y.B., Meng, D.Y., 2013. Sulfated modification and anti-tumor activity of laminarin. Exp. Ther. Med. 6, 1259–1264. https://doi.org/10.3892/etm.2013.1277.
Johnathan, M., Gan, S.H., Ezumi, M.F.W., Faezahtul, A.H., Nurul, A.A., 2016. Phytochemical profiles and inhibitory effects of Tiger Milk mushroom (*Lignosus rhinocerus*) extract on ovalbumin-induced airway inflammation in a rodent model of asthma. BMC Complement Altern. Med. 16. https://doi.org/10.1186/s12906-016-1141-x.
Kalyoncu, F., Oskay, M., Sağlam, H., Erdoğan, T.F., Tamer, A.U., 2010. Antimicrobial and antioxidant activities of mycelia of 10 wild mushroom species. J. Med. Food 13, 415–419. https://doi.org/10.1089/jmf.2009.0090.
Kim, Y., Kim, E., Cheong, C., Williams, D.L., 2000. Structural Characterization of β-D-(1 → 3, 1 → 6)-linked Glucans Using NMR Spectroscopy, 328. pp. 331–341.
Kofuji, K., Aoki, A., Tsubaki, K., Konishi, M., Isobe, T., Murata, Y., 2012. Antioxidant activity of β -glucan. ISRN Pharm 1–5 2012. https://doi.org/10.5402/2012/125864.
Komura, D.L., Ruthes, A.C., Carbonero, E.R., Alquini, G., Rosa, M.C.C., Sassaki, G.L., Iacomini, M., 2010. The origin of mannans found in submerged culture of basidiomycetes. Carbohydr. Polym. 79, 1052–1056. https://doi.org/10.1016/j.carbpol.2009.10.042.
Kong, B.H., Tan, N.H., Fung, S.Y., Pailoor, J., Tan, C.S., Ng, S.T., 2016. Nutritional composition, antioxidant properties, and toxicology evaluation of the sclerotium of Tiger Milk Mushroom *Lignosus tigris* cultivar. E. Nutr. Res. 36, 174–183. https://doi.org/10.1016/j.nutres.2015.10.004.
Kozarski, M., Klaus, A., Jakovljevic, D., Todorovic, N., Vunduk, J., Petrović, P., Niksic, M., Vrvic, M.M., Van Griensven, L., 2015. Antioxidants of edible mushrooms. Molecules 20, 19489–19525. https://doi.org/10.3390/molecules201019489.
Lai, C.K.M., Wong, K.H., Cheung, P.C.K., 2008. Antiproliferative effects of sclerotial polysaccharides from *Polyporus rhinocerus* cooke (aphyllophoromycetideae) on different kinds of leukemic cells. Int. J. Med. Mushrooms 10, 255–264. https://doi.org/10.1615/IntJMedMushr.v10.i3.60.
Lai, W.H., Salleh, S.M., Daud, F., Zainal, Z., Othman, A.M., Saleh, N.M., 2014. Optimization of submerged culture conditions for the production of mycelial biomass and exopolysaccharides from *Lignosus rhinocerus*. Sains Malays. 43, 73–80. https://doi.org/10.4172/2167-7972.1000107.
Lau, B.F., Abdullah, N., Aminudin, N., 2013. Chemical composition of the tiger's milk mushroom, *Lignosus rhinocerotis* (Cooke) Ryvarden, from different developmental stages. J. Agric. Food Chem. 61, 4890–4897. https://doi.org/10.1021/jf4002507.
Lau, B.F., Abdullah, N., Aminudin, N., Lee, H.B., 2013. Chemical composition and cellular toxicity of ethnobotanical-based hot and cold aqueous preparations of the tiger's milk mushroom (*Lignosus rhinocerotis*). J. Ethnopharmacol. 150, 252–262. https://doi.org/10.1016/j.jep.2013.08.034.
Lau, B.F., Abdullah, N., Aminudin, N., Lee, H.B., Tan, P.J., 2015. Ethnomedicinal uses, pharmacological activities, and cultivation of *Lignosus* spp. (tigeŕs milk mushrooms) in Malaysia - a review. J. Ethnopharmacol. 169, 441–458. https://doi.org/10.1016/j.jep.2015.04.042.
Lau, B.F., Abdullah, N., Aminudin, N., Lee, H.B., Yap, K.C., Sabaratnam, V., 2014. The potential of mycelium and culture broth of *Lignosus rhinocerotis* as substitutes for the naturally occurring sclerotium with regard to antioxidant capacity, cytotoxic effect, and low-molecular-weight chemical constituents. PLoS One 9 (7), e1025. https://doi.org/10.1371/journal.pone.0102509.
Lee, M.L., Tan, N.H., Fung, S.Y., Tan, C.S., Ng, S.T., 2012. The antiproliferative activity of sclerotia of *Lignosus rhinocerus* (tiger milk mushroom). Evidence-based Complement. Altern. Med. 2012. https://doi.org/10.1155/2012/697603.
Lee, S.S., Tan, N.H., Fung, S.Y., Sim, S.M., Tan, C.S., Ng, S.T., 2014. Anti-inflammatory effect of the sclerotium of *Lignosus rhinocerotis* (cooke) ryvarden, the tiger milk mushroom. BMC Complement Altern. Med. 14, 1–8. https://doi.org/10.1186/1472-6882-14-359.
Leskosek-Cukalovic, I., Despotovic, S., Lakic, N., Niksic, M., Nedovic, V., Tesevic, V., 2010. *Ganoderma lucidum* - medical mushroom as a raw material for beer with enhanced functional properties. Food Res. Int. 43, 2262–2269. https://doi.org/10.1016/j.foodres.2010.07.014.
Leung, P.H., Zhao, S., Ho, K.P., Wu, J.Y., 2009. Chemical properties and antioxidant activity of exopolysaccharides from mycelial culture of *Cordyceps sinensis* fungus Cs-HK1. Food Chem. 114, 1251–1256. https://doi.org/10.1016/j.foodchem.2008.10.081.
Lidon, F., Silva, M., 2016. An overview on applications and side effects of antioxidant food additives. Emir. J. Food Agric. 28, 823. https://doi.org/10.9755/ejfa.2016-07-806.
Liu, C., Lin, Q., Gao, Y., Ye, L., Xing, Y., Xi, T., 2007. Characterization and antitumor activity of a polysaccharide from *Strongylocentrotus nudus* eggs. Carbohydr. Polym. 67, 313–318. https://doi.org/10.1016/j.carbpol.2006.05.024.
Liu, X., Zhou, B., Lin, R., Jia, L., Deng, P., Fan, K., Wang, G., Wang, L., Zhang, J., 2010. Extraction and antioxidant activities of intracellular polysaccharide from *Pleurotus* sp. mycelium. Int. J. Biol. Macromol. 47, 116–119. https://doi.org/10.1016/j.ijbiomac.2010.05.012.
Liu, Y., Vidanes, G., Lin, Y.C., Mori, S., Siede, W., 2000. Characterization of a *Saccharomyces cerevisiae* homologue of *Schizosaccharomyces pombe* Chk1 involved in DNA-damage-induced M-phase arrest. Mol. Gen. Genet. 262, 1132–1146. https://doi.org/10.1007/PL00008656.
Liu, Y., Zhang, J., Tang, Q., Yang, Y., Guo, Q., Wang, Q., Wu, D., Cui, S.W., 2014. Physicochemical characterization of a high molecular weight bioactive β-D-glucan from the fruiting bodies of *Ganoderma lucidum*. Carbohydr. Polym. 101, 968–974. https://doi.org/10.1016/j.carbpol.2013.10.024.
Lowman, D.W., West, L.J., Bearden, D.W., Wempe, M.F., Power, T.D., Ensley, H.E., Haynes, K., Williams, D.L., Kruppa, M.D., 2011. New insights into the structure of (1→3,1→6)-β-D-glucan side chains in the *Candida glabrata* cell wall. PLoS One 6. https://doi.org/10.1371/journal.pone.0027614.
Mahapatra, S., Banerjee, D., 2013. Fungal exopolysaccharide: production, composition and applications. Microbiol. Insights 6 MBI.S10957. https://doi.org/10.4137/mbi.s10957.
McCleary, B.V., Draga, A., 2016. Measurement of β-Glucan in mushrooms and mycelial products. J. AOAC Int. 99, 364–373. https://doi.org/10.5740/jaoacint.15-0289.
Miao, M., Li, R., Jiang, B., Cui, S.W., Lu, K., Zhang, T., 2014. Structure and digestibility of endosperm water-soluble α-glucans from different sugary maize mutants. Food Chem. 143, 156–162. https://doi.org/10.1016/j.foodchem.2013.07.109.
Mohanarji, S., Dharmalingam, S., Kalusalingam, A., Science, A., 2012. Screening of *Lignosus rhinocerus* extracts as antimicrobial agents against selected human pathogens. J. Pharm. Biomed. Sci. 18, 1–4.
Munir, N., Sharif, N., Naz, S., Farkhanda, M., 2013. Algae: a potent antioxidant source. Sky J Microbiol Res 1, 22–31.
Nallathamby, N., Phan, C.W., Seow, S.L.S., Baskaran, A., Lakshmanan, H., Abd Malek, S. N., Sabaratnam, V., 2018. A status review of the bioactive activities of tiger milk mushroom *Lignosus rhinocerotis* (Cooke) Ryvarden. Front. Pharmacol. 8, 998. https://doi.org/10.3389/fphar.2017.00998.
Nie, S.P., Cui, S.W., Phillips, A.O., Xie, M.Y., Phillips, G.O., Al-Assaf, S., Zhang, X.L., 2011. Elucidation of the structure of a bioactive hydrophilic polysaccharide from *Cordyceps sinensis* by methylation analysis and NMR spectroscopy. Carbohydr. Polym. 84, 894–899. https://doi.org/10.1016/j.carbpol.2010.12.033.

Núñez, M., Ryvarden, L., 2001. East asian polypores. Synopsis Fungorum 14, 170–522.
Paulo, E.M., Boffo, E.F., Branco, A., Valente, Â.M.M.P., Melo, I.S., Ferreira, A.G., Roque, M.R.A., de Assis, S.A., 2012. Production, extraction and characterization of exopolysaccharides produced by the native *Leuconostoc pseudomesenteroides* R2 strain. An. Acad. Bras. Cienc. 84, 495–507. https://doi.org/10.1590/S0001-37652012000200018.
Pomin, V.H.. London: IntechOpen 64–98. https://doi.org/10.5772/48136.
Prado, B.M., Kim, S., Özen, B.F., Mauer, L.J., 2005. Differentiation of carbohydrate gums and mixtures using fourier transform infrared spectroscopy and chemometrics. J. Agric. Food Chem. 53, 2823–2829. https://doi.org/10.1021/jf0485537.
Rabha, B., Nadra, R., Ahmed, B., 2012. Effect of some fermentation substrates and growth temperature on exopolysaccharide production by *Streptococcus thermophilus* BN1. Int. J. Biosci. Biochem. Bioinforma. 2, 2–5.
Rop, O., Mlcek, J., Jurikova, T., 2009. Beta-glucans in higher fungi and their health effects. Nutr. Rev. 67, 624–631. https://doi.org/10.1111/j.1753-4887.2009.00230.x.
Ruthes, A.C., Carbonero, E.R., Córdova, M.M., Baggio, C.H., Santos, A.R.S., Sassaki, G.L., Cipriani, T.R., Gorin, P.A.J., Iacomini, M., 2013. *Lactarius rufus* (1→3),(1→6)-β-d-glucans: structure, antinociceptive and anti-inflammatory effects. Carbohydr. Polym. 94, 129–136. https://doi.org/10.1016/j.carbpol.2013.01.026.
Sathiyanarayanan, G., Dineshkumar, K., Yang, Y.H., 2017. Microbial exopolysaccharide-mediated synthesis and stabilization of metal nanoparticles. Crit. Rev. Microbiol. 43, 731–752. https://doi.org/10.1080/1040841X.2017.1306689.
Sims, I.M., Carnachan, S.M., Bell, T.J., Hinkley, S.F.R., 2018. Methylation analysis of polysaccharides: technical advice. Carbohydr. Polym. 188, 1–7. https://doi.org/10.1016/j.carbpol.2017.12.075.
Sotome, K., Hattori, T., Ota, Y., To-anun, C., Salleh, B., Kakishima, M., 2008. Phylogenetic relationships of *Polyporus* and morphologically allied genera. Mycologia 100, 603–615. https://doi.org/10.3852/07-191R.
Sulaiman, S.F., Ooi, K.L., 2012. Polyphenolic and vitamin C contents and antioxidant activities of aqueous extracts from mature-green and ripe fruit fleshes of *Mangifera* sp. J. Agric. Food Chem. 60, 11832–11838. https://doi.org/10.1021/jf303736h.
Supramani, S., Ahmad, R., Ilham, Z., Annuar, M.S.M., Klaus, A., Wan-Mohtar, W.A.A.Q. I., 2019. Optimisation of biomass, exopolysaccharide and intracellular polysaccharide production from the mycelium of an identified *Ganoderma lucidum* strain qrs 5120 using response surface methodology. AIMS Microbiol 5, 19–38. https://doi.org/10.3934/microbiol.2019.1.19.
Supramani, S., Jailani, N., Ramarao, K., Mohd Zain, N.A., Klaus, A., Ahmad, R., Wan-Mohtar, W.A.A.Q.I., 2019. Pellet diameter and morphology of European *Ganoderma pfeifferi* in a repeated-batch fermentation for exopolysaccharide production. Biocatal. Agric. Biotechnol. 19. https://doi.org/10.1016/j.bcab.2019.101118.
Synytsya, A., Novak, M., 2014. Structural analysis of glucans. Ann. Transl. Med. 2, 1–14. https://doi.org/10.3978/j.issn.2305-5839.2014.02.07.
Tada, R., Adachi, Y., Ishibashi, K., Ohno, N., 2009. An unambiguous structural elucidation of a 1,3-β-d-glucan obtained from liquid-cultured *Grifola frondosa* by solution NMR experiments. Carbohydr. Res. 344, 400–404. https://doi.org/10.1016/j.carres.2008.11.005.
Tamura, K., Stecher, G., Peterson, D., Filipski, A., Kumar, S., 2013. MEGA6: molecular evolutionary genetics analysis version 6.0. Mol. Biol. Evol. 30, 2725–2729. https://doi.org/10.1093/molbev/mst197.
Tan, C.S., Ng, S.T., Tan, J., 2013. Two new species of *Lignosus* (Polyporaceae) from Malaysia - *L. tigris* and *L. cameronensis*. Mycotaxon 123, 193–204. https://doi.org/10.5248/123.193.
Vasavi, Y., Parthiban, C., Sathis Kumar, D., Banji, D., Srisutherson, N., Ghosh, S., Vinay Kumar Chakravarthy, M., 2011. Heteronuclear multible bond correlation spectroscopy- an overview. Int. J. PharmTech Res. 3, 1410–1422.
Wagner, R., Mitchell, D.A., Sassaki, G.L., Lopes de Almeida Amazonas, M.A., Berovi, M., 2003. Current techniques for the cultivation of *Ganoderma lucidum* for the production of biomass. Ganoderic Acid and Polysaccharides 41, 371–382.
Wan-Mohtar, W.A.A.Q.I., Ab Kadir, S., Saari, N., 2016. The morphology of *Ganoderma lucidum* mycelium in a repeated-batch fermentation for exopolysaccharide production. Biotechnol. Reports 11, 2–11. https://doi.org/10.1016/j.btre.2016.05.005.
Wan-Mohtar, W.A.A.Q.I., Mahmud, N., Supramani, S., Ahmad, R., Zain, N.A.M., Hassan, N.A.M., Peryasamy, J., Halim-Lim, S.A., 2018. Fruiting-body-base flour from an oyster mushroom-a waste source of antioxidative flour for developing potential functional cookies and steamed-bun. AIMS Agric. Food 3, 481–492. https://doi.org/10.3934/AGRFOOD.2018.4.481.
Wan-Mohtar, W.A.A.Q.I., Viegelmann, C., Klaus, A., Lim, S.A.H., 2017. Antifungal-demelanizing properties and RAW264.7 macrophages stimulation of glucan sulfate from the mycelium of the mushroom *Ganoderma lucidum*. Food Sci. Biotechnol. 26, 159–165. https://doi.org/10.1007/s10068-017-0021-6.
Wan-Mohtar, W.A.A.Q.I., Young, L., Abbott, G.M., Clements, C., Harvey, L.M., McNeil, B., 2016. Antimicrobial properties and cytotoxicity of sulfated (1,3)-β-D-glucan from the mycelium of the mushroom *Ganoderma lucidum*. J. Microbiol. Biotechnol. 26, 999–1010. https://doi.org/10.4014/jmb.1510.10018.
Wang, J., Zhang, L., 2009. Structure and chain conformation of five water-soluble derivatives of a β-d-glucan isolated from *Ganoderma lucidum*. Carbohydr. Res. 344, 105–112. https://doi.org/10.1016/j.carres.2008.09.024.
Wong, K.H., Lai, C.K.M., Cheung, P.C.K., 2011. Immunomodulatory activities of mushroom sclerotial polysaccharides. Food Hydrocolloids 25, 150–158. https://doi.org/10.1016/j.foodhyd.2010.04.008.
Wu, D., Tang, C., Liu, Y., Li, Q., Wang, W., Zhou, S., Zhang, Z., Cui, F., Yang, Y., 2019. Structural elucidation and immunomodulatory activity of a β-D-glucan prepared by freeze-thawing from *Hericium erinaceus*. Carbohydr. Polym. 222. https://doi.org/10.1016/j.carbpol.2019.114996.
Yang, H., Min, W., Bi, P., Zhou, H., Huang, F., 2013. Stimulatory effects of *Coix lacryma-jobi* oil on the mycelial growth and metabolites biosynthesis by the submerged culture of Ganoderma lucidum. Biochem. Eng. J. 76, 77–82. https://doi.org/10.1016/j.bej.2013.04.012.
Yap, H.Y.Y., Chooi, Y.H., Firdaus-Raih, M., Fung, S.Y., Ng, S.T., Tan, C.S., Tan, N.H., 2014. The genome of the Tiger Milk mushroom, *Lignosus rhinocerotis*, provides insights into the genetic basis of its medicinal properties. BMC Genomics 15. https://doi.org/10.1186/1471-2164-15-635.
Yap, H.Y.Y., Tan, N.H., Ng, S.T., Tan, C.S., Fung, S.Y., 2018. Inhibition of protein glycation by tiger milk mushroom [*Lignosus rhinocerus* (Cooke) Ryvarden] and search for potential anti-diabetic activity-related metabolic pathways by genomic and transcriptomic data mining. Front. Pharmacol. 9. https://doi.org/10.3389/fphar.2018.00103.
Yap, Y.H., Tan, N., Fung, S., Aziz, A.A., Tan, C., Ng, S., 2013. Nutrient composition, antioxidant properties, and anti-proliferative activity of *Lignosus rhinocerus* Cooke sclerotium. J. Sci. Food Agric. 93, 2945–2952. https://doi.org/10.1002/jsfa.6121.